Spatial transcriptome of a germinal center plasmablastic burst hints at *MYD88*/*CD79B* mutants-enriched diffuse large B-cell lymphomas

Vincenzo L'Imperio[1*], Gaia Morello[2*], Maria Carmela Vegliante[3], Valeria Cancila[2], Giorgio Bertolazzi[2], Saveria Mazzara[4], Beatrice Belmonte[2], Alessandro Mangogna[5], Piera Balzarini[6], Lilia Corral[7], Gianluca Lopez[8], Arianna Di Napoli[8], Fabio Facchetti[9], Fabio Pagni[1#], Claudio Tripodo[2,10#]

Supplementary Materials

Supplemental Table S1. List of the 54 genes recurrently mutated in lymphomas included in the targeted NGS panel.

Supplemental Table S2. Targeted NGS of 54 genes recurrently mutated in lymphomas performed on the microdissected GEx GC.

Supplemental Table S3. Expression of 1824 genes over 24 ROIs obtained through GeoMx Digital Spatial Profiler of NanoString. NanoString has performed the Q3 normalization.

Supplemental Table S4. Differentially expressed genes among DZ, LZ, PERI and GEx ROI types (Kruskal-Wallis adjusted p-values < 0.05) and relative gene set enrichment analysis (KEGG, Reactome Pathway, and GO-BP libraries).

Supplemental Table S5. Average SpatialDecon cell fraction estimations over 24 DZ, LZ, PERI and GEx ROIs. Kruskal-Wallis test has been used to compare cell fraction distributions among ROIs.

Supplemental Table S6. Fisher exact test p-values from enrichment analysis on cluster 1 and cluster 2 among cell of origin categories in DLBCL cases relative to the Schmitz *et al*. dataset (6).

Supplemental Table S7. Fisher exact test p-values from enrichment analysis on cluster 1 and cluster 2 among genetic subtype categories in DLBCL cases relative to the Schmitz *et al*. dataset (6).

Supplemental Table S8. Pairwise comparisons of average GEx signature scores over genetic subtype categories in DLBCL cases relative to the Schmitz *et al*. (6) and Chapuy *et al*. (5) datasets through Bootstrap t-test.

Supplemental Table S9. Average CIBERSORTx cell fraction estimations over cluster 1 and cluster 2 DLBCL cases relative to the Schmitz *et al*. dataset (6). Wilcoxon-Mann-Whitney test has been used to compare cell fraction distributions among clusters.

Supplementary Data

Supplementary Figure S1. Immunostaining for HHV8 (Original magnifications x50, inset x200) (**A**) and EBER in situ hybridization (Original magnifications x50, inset x200) (**B**) were negative in the described germinotropic expansion of the tonsil (asterisk).

Supplementary Figure S2. A-B, PCR-based gene scan clonality analysis with master mixes targeting the framework 1, 2, 3 (FR) and the joining region (J) (**A**) or the diversity (D) regions

with the joining region (J) (**B**) of the IGH locus showed a polyclonal rearrangement of the IGH gene in both the sample and the polyclonal control, whereas a clonal peak (arrow) was present in the monoclonal control. **C**, Similarly, the sample showed a polyclonal rearrangement in both the multiplex PCR targeting the variable (V) and the joining (J) regions or the deleting element (Kde) with the variable (V) or intragenic Jκ-Cκ regions of the IGK chain locusH.

Supplementary Figure S3. Fluorescent in situ hybridization using an IRF4/DUSP22 break apart probe indicates the absence of gene rearrangements (two red and green fusion-signals in the majority of the cells).

Supplementary Figure S4. Heatmap of the average gene expression of 10 marker genes selected according to Figure 1B immunophenotypical analyses of the DZ, LZ, Peri, and GEx ROIs.

Supplementary Figure S5. A, Comparative analysis of CD138, IRF4 and CD3 IHC markers in 24 ROIs in the profiled GEx, DZ, LZ and Peri regions. **B**, Heatmap of the expression of the quantitative immunohistochemical analysis of CD3, CD138, and IRF4 markers evaluated in the DZ, LZ, PERI, and GEx regions. The bootstrap t-test has been used to compare GEx ROIs with others.

Supplementary Figure S6. A, Cumulative distributions of the 17 genes GEx signature expression per patient among the two groups (Kolmogorov-Smirnov p-value < 10e-16). **B**, Overall survival of the two groups of BLBCL cases obtained from the unsupervised clustering of the Schmitz *et al*. dataset (6). **C**, Progression free survival of the two clusters obtained from the unsupervised clustering. **D-E**, GEx score distribution over genetic subtypes categories in

Schmitz *et al*. (6) (D) and Chapuy *et al*. (5) (E) datasets. The GEx score has been calculated as the difference between the sum of GEx-UP gene expression and the sum of GEx-DOWN gene expression. The bootstrap t-test has been used to compare the average values (rhomboid points) among the genetic subtypes categories.

Supplementary Figure 1

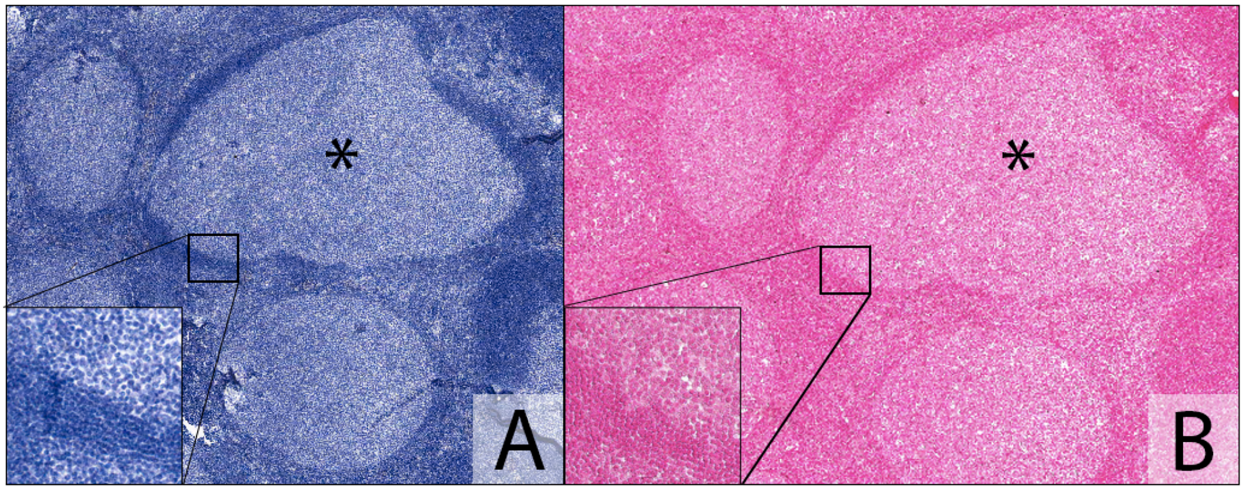

Supplementary Figure 2

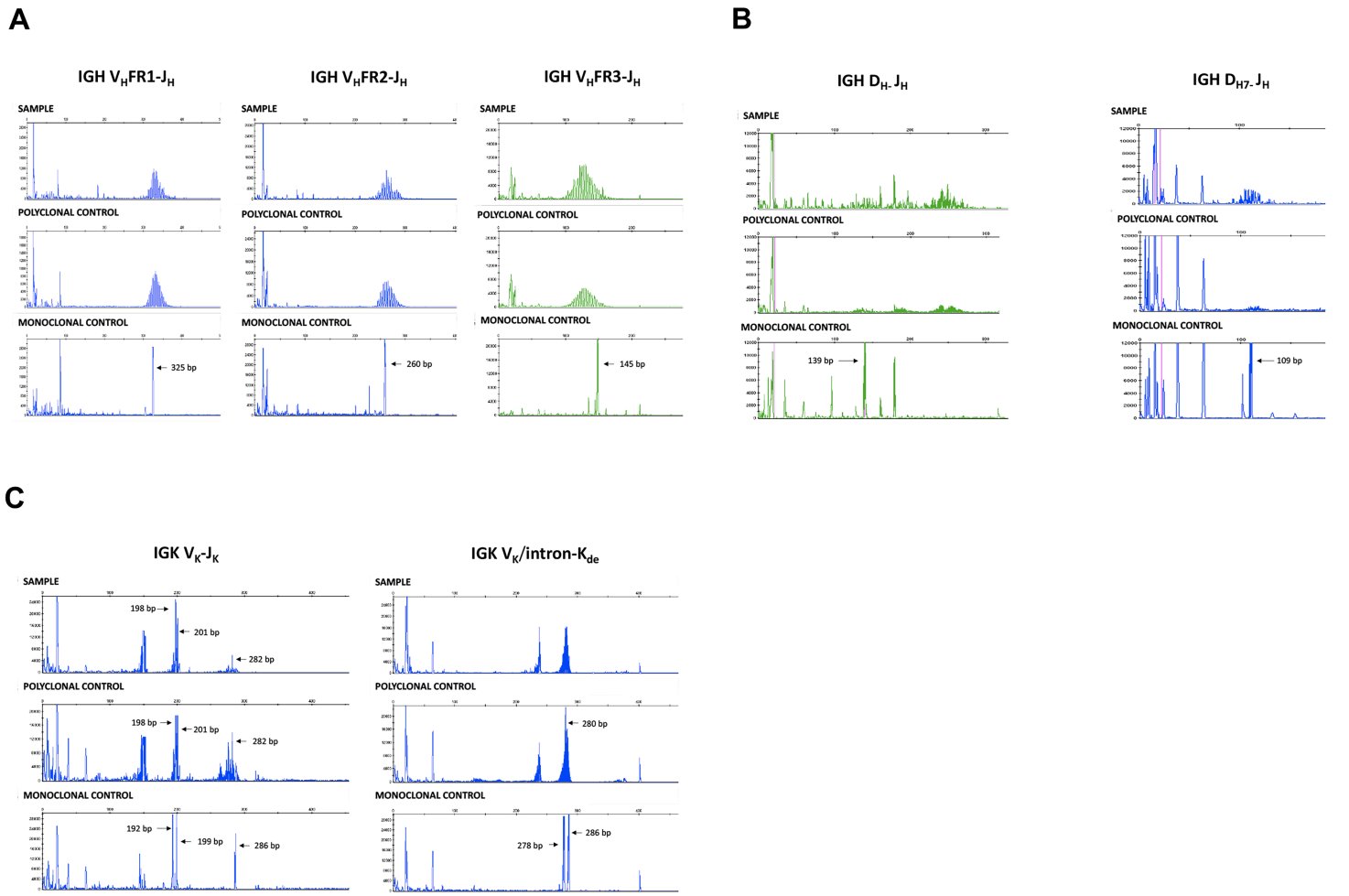

Supplementary Figure 3

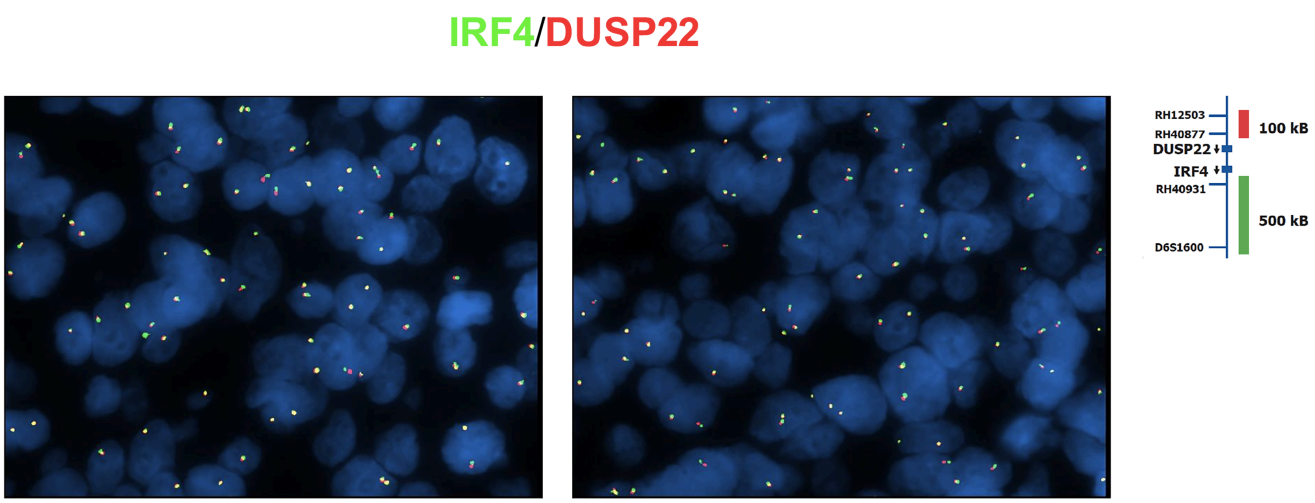

Supplementary Figure 4

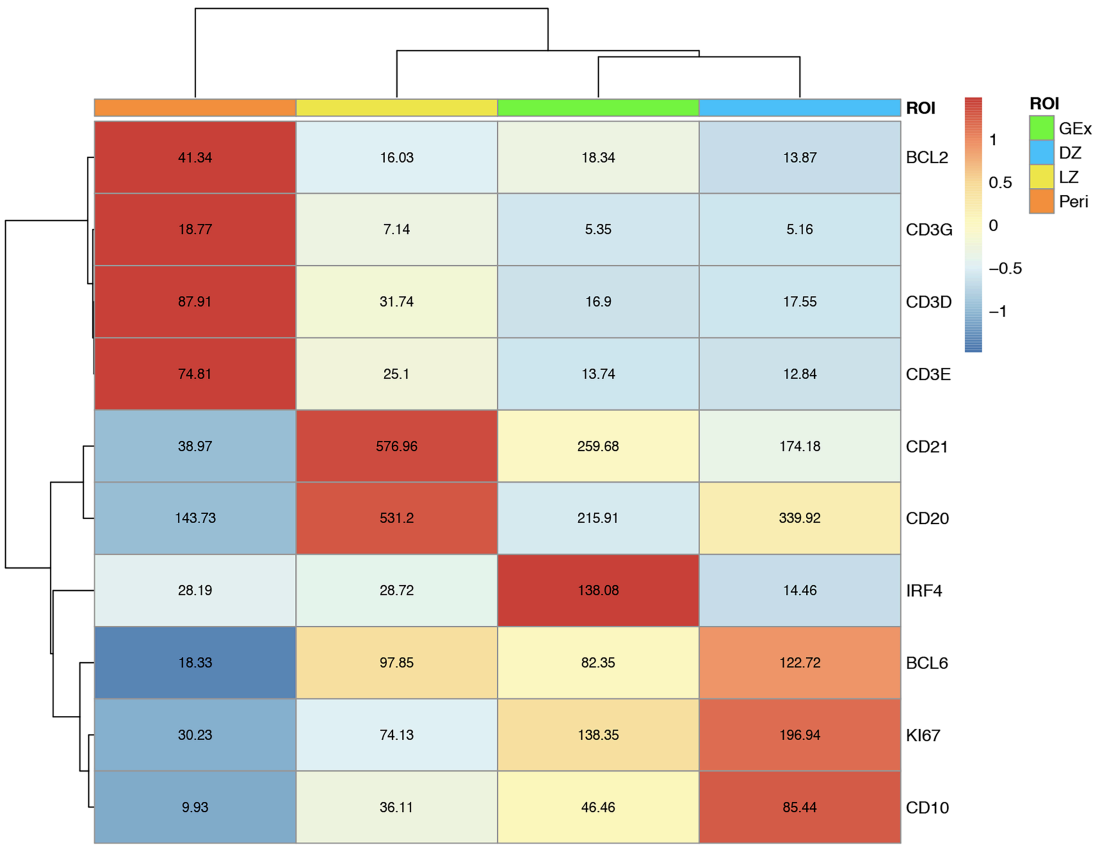

Supplementary Figure 5

A

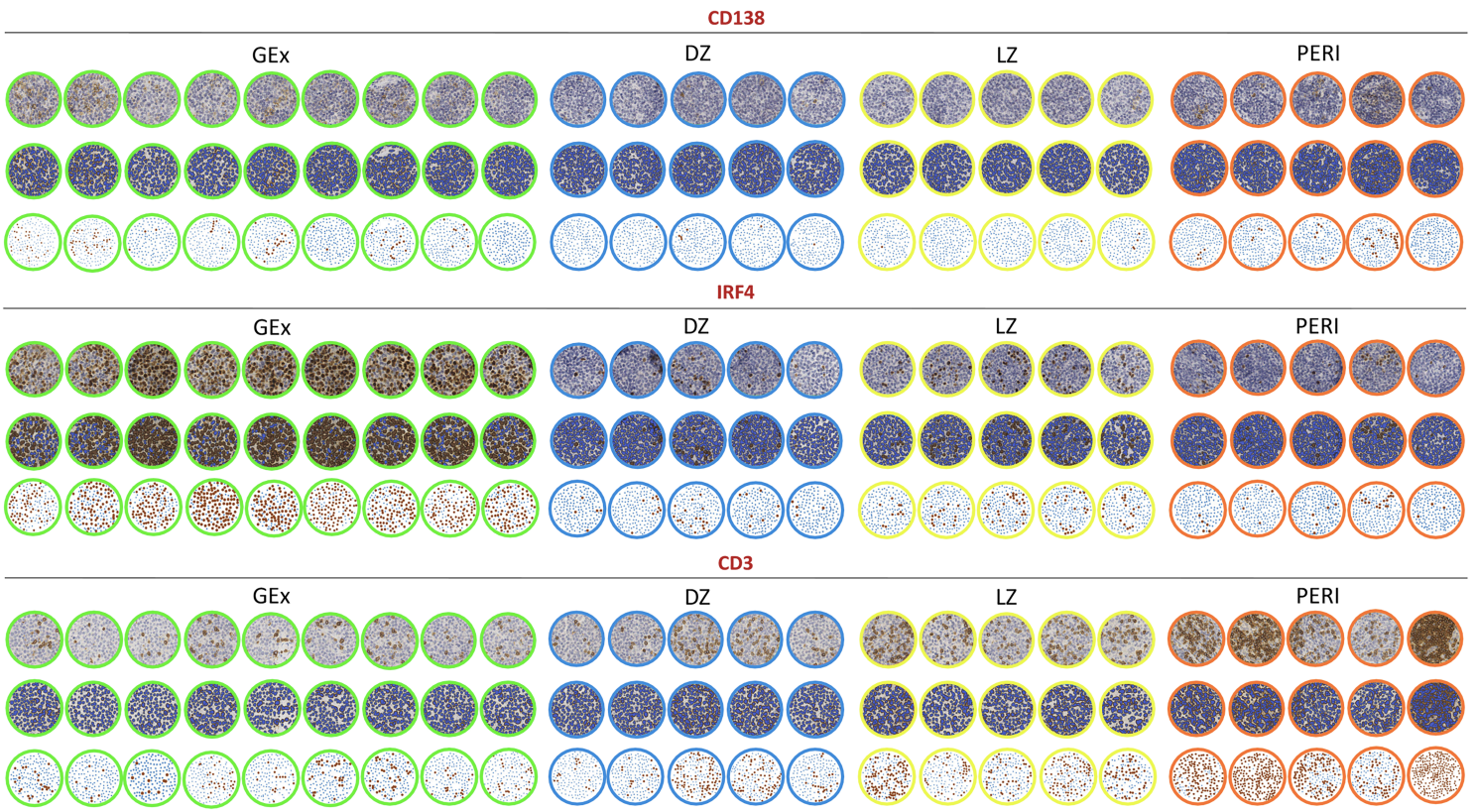

B

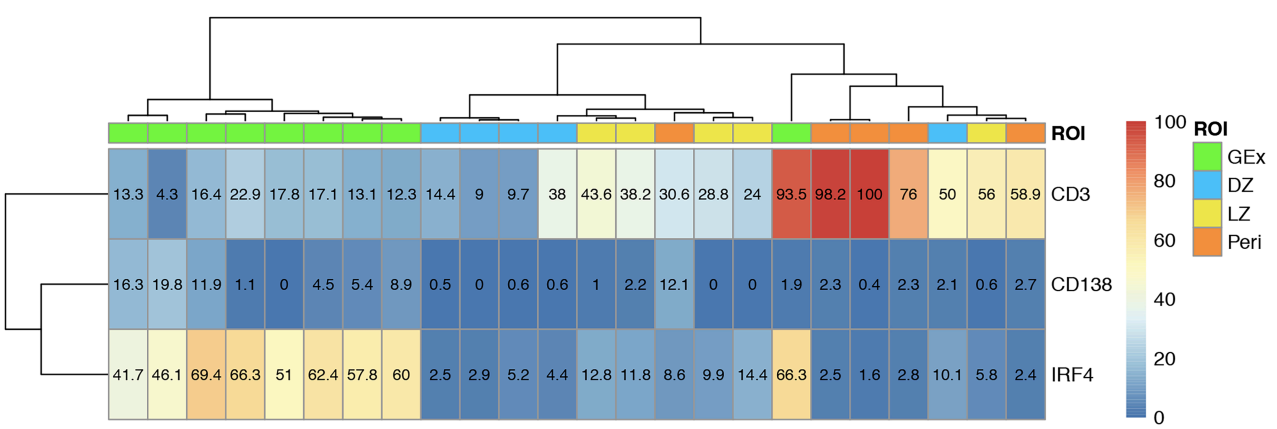

	gene	logFC	pval
1	IRF4	3.15	<2e−04
2	CD138	2.09	0.0462
3	CD3	−0.94	0.0986

Supplementary Figure 6